
In-Flight Evaluation of Aerodynamic Predictions of an Air-Launched Space Booster

Robert E. Curry, Michael R. Mendenhall, and Bryan Moulton

April 1992



National Aeronautics and
Space Administration

In-Flight Evaluation of Aerodynamic Predictions of an Air-Launched Space Booster

Robert E. Curry
NASA Dryden Flight Research Facility, Edwards, California

Michael R. Mendenhall
Nielsen Engineering & Research, Inc., Mountain View, California

Bryan Moulton
PRC Inc., Edwards, California

1992



National Aeronautics and
Space Administration

Dryden Flight Research Facility
Edwards, California 93523-0273

IN-FLIGHT EVALUATION OF AERODYNAMIC PREDICTIONS OF AN AIR-LAUNCHED SPACE BOOSTER

Robert E. Curry

NASA Dryden Flight Research Facility

P.O. Box 273

Edwards, CA 93523 - 0273, USA

Michael R. Mendenhall

Nielsen Engineering & Research, Inc.

510 Clyde Avenue

Mountain View, CA 94043, USA

Bryan Moulton

PRC Inc.

Edwards, CA 93523-0273 USA

SUMMARY

Several analytical aerodynamic design tools that were applied to the Pegasus® air-launched space booster were evaluated using flight measurements. The study was limited to existing codes and was conducted with limited computational resources. The flight instrumentation was constrained to have minimal impact on the primary Pegasus missions.

Where appropriate, the flight measurements were compared with computational data. Aerodynamic performance and trim data from the first two flights were correlated with predictions. Local measurements in the wing and wing-body interference region were correlated with analytical data. This complex flow region includes the effect of aerothermal heating magnification caused by the presence of a corner vortex and interaction of the wing leading edge shock and fuselage boundary layer.

The operation of the first two missions indicates that the aerodynamic design approach for Pegasus was adequate, and data show that acceptable margins were available. Additionally, the correlations provide insight into the capabilities of these analytical tools for more complex vehicles in which design margins may be more stringent.

NOMENCLATURE

C_D drag coefficient

C_L lift coefficient

C_m	pitching moment coefficient
CFD	computational fluid dynamics
c.g.	center of gravity
FS	fuselage station, measured in forward direction, in.
h_p	pressure altitude, ft (m)
HTRSI	high-temperature reusable surface insulation
M	Mach number
$\frac{p}{p_R}$	local pressure divided by pressure measured at reference location (FS = 288.4 in., z = 17 in.)
\bar{q}	dynamic pressure, lb/ft^2 (kPa)
$\frac{q}{q_R}$	local convective heating rate divided by rate measured at reference location (FS = 288.4 in., z = 17 in.)
Re	unit Reynolds number, $\text{ft}^{-1} (\text{m}^{-1})$
T	temperature, °F (°C)
TPS	thermal protection system
y	lateral coordinate measured from vehicle centerline, in.
z	vertical coordinate measured from vehicle centerline, in.
α	angle of attack, deg
β	angle of sideslip, deg
Δ	incremental change
δR	rudder deflection, deg

® Pegasus is a registered trademark of Orbital Sciences Corp., Fairfax, VA.

INTRODUCTION

In recent years, computational aerodynamic methods have played a more significant role in developing hypersonic flight vehicles. Two reasons are the potential cost savings from reduced ground test requirements and the need for design data at conditions which cannot be fully simulated in wind-tunnel facilities. The usefulness of such methods depends on two issues: their ability to represent important physical phenomena and their practicality (i.e., application effort and resource requirements) in the design process. To assess the first issue, the code validation process, requires a series of highly controlled experiments with extensive measurement surveys as discussed in Ref. 1. The issue of the practical nature of such methods, however, must be assessed with respect to the design of actual flight vehicles. Few opportunities have arisen for this type of evaluation.

The Pegasus® air-launched space booster system offered an opportunity to conduct such an evaluation. This vehicle was developed as a commercial joint venture by Orbital Sciences Corp., Fairfax, VA, and Hercules Aerospace Corp., Magna, UT, to deliver small payloads into orbit. In addition to the primary payload, some limited additional instrumentation was installed on the first two flights for research. This instrumentation had minimal impact on the orbital delivery mission and, therefore, was accommodated at low cost.

Several features of the Pegasus vehicle made it attractive for this research approach. Pegasus uses wing and tail surfaces for lift, stability, and control at speeds up to Mach 8. These surfaces generate interesting hypersonic flow fields for analysis and provide convenient locations for instrumentation. Because of the multi-stage design, the weight of additional research hardware on the first stage had small impact on the payload performance of the overall system (the ratio of additional first-stage weight to reduced payload capability was about 18:1).

In addition to these benefits, a significant analytical database existed for the Pegasus. The original aerodynamic design was developed exclusively through computational design tools by Nielsen Engineering & Research, Inc., Mountain View, CA. This approach and the resulting data are described in detail in Ref. 2. The resulting database was obtained from existing codes and methods which could be applied within the cost and manpower constraints of the project. The design effort concentrated on the requirements for vehicle

development and not with the intent to develop codes or theory.

In addition to the design effort, some postflight computations were conducted to enhance the value of the flight data. All analytical results discussed in this report, however, represent a level of sophistication and application effort typical of the privately funded Pegasus design effort.

The objective of this study was to evaluate certain aspects of code performance with measurements from the first two flights. Specifically, this includes correlations of first-stage vehicle aerodynamics (performance and trim) at high speeds and local aerodynamics on the wing and in the wing root interference region. The evaluation includes analytical data from both the pre-flight and follow-on computational efforts. Many aspects of the extensive analytical design process (such as launch dynamics, exhaust-plume-induced separation studies, fin actuator heating, etc) could not be assessed with the available flight data and, therefore, will not be addressed in this paper.

This paper will describe the various flight and analytical data sources and their limitations. The correlations will be considered with respect to the relatively conservative Pegasus requirements and also with respect to more complex vehicles which may have less design margin.

A series of more sophisticated hypersonic flight experiments to be conducted using the Pegasus is under development. The series will use a stand-alone data acquisition system and an aerodynamically smooth wing test panel. These experiments will build on the minimal-impact, add-on, flight-research approach developed in the current research.

BASELINE VEHICLE DESCRIPTION AND OPERATION

The Pegasus is a three-stage, solid-rocket space launch vehicle designed to insert small payloads, 600 to 1000 lb (270 to 450 kg), into orbit, (Ref. 3). Figure 1 shows the configuration. The configuration has a cylindrical fuselage and high wing with clipped-delta planform. A large fairing, referred to as the fillet, extends along the wing-body intersection. The wing and tail surfaces are part of the first stage. The aerodynamic surfaces are fabricated primarily from graphite-epoxy structures and covered with thermal protection materials. The thermal protection system (TPS) includes layers of insulating material and ablatives. The vehicle

has an autonomous onboard guidance and control system. The flight 1 and 2 vehicles had virtually identical external configurations. Key physical characteristics of Pegasus follow:

Wing reference area	145.4 ft ² (13.51 m ²)
Span	22 ft (6.7 m)
Mean aerodynamic chord	8.14 ft (2.48 m)
Root chord	12.11 ft (3.69 m)
Tip chord	1.11 ft (0.338 m)
Aspect ratio	3.33
Wing leading edge sweep	45°
Wing leading edge radius	1 in. (0.0254 m)
Fuselage length overall	49.34 ft (15.0 m)
Fuselage nominal diameter	4.17 ft (1.27 m)

The Pegasus vehicle is carried aloft under the wing of a B-52 aircraft, and is air-launched at an altitude of about 42,000 ft (12.8 km) and Mach 0.8. Approximately 5 sec after release, the first-stage motor is ignited and the vehicle accelerates to a Mach number of about 8 and an altitude of about 210,000 ft (64 km). During this first-stage operation, which lasts about 80 sec, the vehicle is aerodynamically controlled by all-moving tail surfaces. A 2.5-g pull-up is initiated early in the flight to achieve the desired flightpath angle. The *g*-level is gradually reduced so that the vehicle is nominally at 0° angle of attack at Mach numbers of 5 and above. During the final seconds of the first-stage flight, small solid-rocket motors in the movable tail surfaces are ignited to augment control at low-dynamic pressure conditions. After burnout, the vehicle coasts for several seconds before stage separation. After separation, the stages are not recovered.

FLIGHT TEST DATA

Data from the first two flights of the Pegasus were used in this study. The intent to have minimal impact on the primary satellite deployment missions was a significant challenge to the research effort. The sensors were constrained to have little structural design impact, data were acquired through the baseline Pegasus systems which had additional limitations, and the trajectories were fixed by the requirements of the primary mission payloads. More information about the flight test procedures and data can be obtained from Refs. 4 through 6 and a later publication.*

Instrumentation

Flight data were derived from the baseline Pegasus flight instrumentation as well as from additional research instrumentation. The baseline flight instrumentation included onboard control surface position and inertial navigation system data, ground-based radar data, and weather observations.

Additional research instrumentation on flight 1 included conventional thermocouples which were installed on nonablating plugs and thin-foil thermocouples. The 1-in. diameter nonablating plugs were fabricated from high-temperature reusable surface insulation (HRSI) material with a high-emissivity coating. The HRSI plug surface temperatures were significantly different from the surrounding structure but were highly responsive to changes in the local flow characteristics. Ten HRSI plugs were installed on the right fillet sidewall. Seventy-six foil gauges were distributed in two rows on the right wing lower surface and leading edge, and at various locations on the right fillet sidewall. These foils were approximately 0.006-in. thick and were inserted between layers of the TPS during fabrication. Certain locations had more than one gauge inserted at different depths of the TPS. The TPS consisted of layers of insulative material and a spray-on ablative and in these regions had a nominal thickness of about 0.06 in. (1.5 mm). The foil-gauge installation resulted in only minor distortion of the thermal properties of the surrounding structure. On the other hand, these gauges were covered by a low-temperature ablative and not directly exposed to the flow. As a result, they were of limited value in studying local flow phenomena. Figures 2(a) and 2(b) show a layout of the flight-1 instrumentation.

The flight-2 vehicle accommodated 8 HRSI plugs, 8 surface pressures, 7 commercially available calorimeters, and 14 foil thermocouples. The flush pressure measurement ports were installed on selected HRSI plugs. All flight-2 instrumentation was located on the right fillet sidewall, as shown in Fig. 2(c).

All onboard measurements were obtained through the baseline Pegasus data processing system. In addition to data acquisition, this 8-bit system provided all flight-control, guidance, and vehicle-management functions. For both flights, the research instrumentation bandwidth portion of this system was limited to approximately 3000 bit/sec. The system had fixed frame rates with a maximum of 25 samples/sec. All onboard data were telemetered to ground stations as a pulse-code-modulated signal.

*Proposed NASA Technical Memorandum by Noffz, Moes, Haering, and Kolodziej.

Data Reduction

Flight conditions along the trajectory were estimated from a combination of radar tracking from up to eight sites and the onboard inertial measurements using a weighted least-squares method and an atmospheric model. The atmospheric model was determined from a combination of weather observations including balloon data, launch aircraft measurements, stratospheric charts, and climatological databases. This model was also used to correct for radar refraction. The trajectory analysis was adversely affected by the low radar tracking angles (which resulted in high sensitivity to atmospheric refraction modeling) and the large geographic range covered during the first-stage flight.

The vehicle aerodynamic forces and moments were derived by balancing the measured body axis accelerations with vehicle properties. The mass and inertias were estimated from preflight measurements and the expected propellant loss during rocket motor burn. Thrust was modeled as a function of time using data from ground tests corrected for ambient pressure at altitude. Fin rocket thrust was also modeled as a function of time. Total rocket thrust was assumed to be longitudinally aligned and subtracted from the net axial force to determine the aerodynamic component of axial force. Lift and drag were determined from the normal and axial force components and the derived angle of attack. The lift, drag, and pitching moments were converted to coefficient form using wing reference dimensions and dynamic pressure. The pitching moment was referenced to the modeled flight center-of-gravity (c.g.) location. The accuracy of these terms is largely dependent on the accuracy of the estimated trajectory and meteorological reconstruction which may vary from flight to flight. The repeatability of results over a series of future flight dates should identify any significant errors if they exist.

At high altitudes, as dynamic pressure diminishes, small misalignment errors in the thrust axis result in large surface trim requirements. Since these trim requirements are primarily thrust related and not aerodynamic, moment data at these times cannot be expected to correlate well with aerodynamic predictions. This effect can be identified by elevator and rudder deflections (rudder data are shown in Fig. 3) which vary proportionately to the reduction in free-stream dynamic pressure and end with motor burn-out. The orientation and magnitude of the thrust misalignment vary between vehicles. As a result, moment measurements were limited to Mach numbers of about 5 or below. A

control-system-induced oscillation occurred on flight 1 which contaminated the linear acceleration measurements. This limited the usable range of lift and drag data to Mach numbers less than 4.5. This problem was eliminated on flight 2.

Convective heat-flux estimates were derived postflight from the various thermocouple installations. The foil thermocouples located in the leading edge TPS were analyzed using an inverse analysis method, Ref. 7. In this study, the results are only considered as an indication of relative heating rate distribution. This approach is only valid prior to the onset of ablation. Convective heat flux was derived from the HRSI plug temperatures using a one-dimensional model and finite element thermal resistance analogy method. These computations are sensitive to the modeling of material properties, sensor installation, and emissivity. No attempt was made to account for the local surface temperature perturbations caused by the plugs or for ablation products in the boundary layer. As a result, the absolute value of heating rate from this derivation is not considered representative of Pegasus surface heating; however, the data are indicative of relative heating characteristics. Relative heating rates in the fillet region are defined as the local value divided by the value obtained on the lower, forward region of the fillet, as shown on Fig. 2. As noted in Ref. 4, this location is expected to be forward of the intersecting wing shock location and is, therefore, felt to represent a suitable reference condition.

Trajectories

Figure 4 shows flight-trajectory parameters for the two flights. Differences in the trajectories were primarily caused by requirements of the satellite payloads. Both flights achieved a maximum angle of attack of about 20°; flight 1 then stabilized briefly at about 7.5°, and flight 2 stabilized at about 2.5°. The angle of attack for both vehicles was about 0° for Mach numbers of 5 and higher. Flight 2 experienced higher dynamic pressures, but both were generally in the ideal gas flight regime.

ANALYTIC DATA

Force and Moment Aero Models

A six-degree-of-freedom model of the vehicle forces and moments was developed for conditions throughout the flight envelope. The coefficient data include the effects of Mach, angles of attack and sideslip, control surface deflection, and angular rates. Development of this aero model was a major accomplishment of the

Pegasus development effort and is described in detail in Ref. 2. It relied primarily on a variety of semi-empirical database and panel methods; however, advanced computational methods (for example, Euler and Navier-Stokes) were used for selected studies throughout the design and analysis. The computational resources for this effort were not severe by modern standards, but the overall size of the data sets (504 longitudinal and 918 lateral flow conditions) indicates the level of analysis effort required. Approximately four times this number of flow conditions were studied because of design iterations and configuration changes. This data set was used to support preliminary design, performance studies, structural loading predictions, and guidance and control law simulation and development.

The aero model data shown in this report were obtained by applying the flight-estimated altitude, angle of attack, dynamic pressure, and control surface time histories to the database and correcting for modeled c.g. position. The resulting lift, drag, and pitching moment coefficients, therefore, can be directly correlated with flight values.

Computational Fluid Dynamics (CFD)

Flow-field solutions for the Pegasus configuration were obtained at a selected set of flight conditions as shown in Fig. 5.

The F3D code was utilized by Nielsen Engineering & Research, Inc., during the design effort prior to flight 1 to assess flow quality in the vicinity of the fillet and to corroborate aero load predictions. Additional F3D solutions were obtained after flight 1 at specific free-stream conditions encountered on the flight. The code solves the compressible three-dimensional, thin-layer Navier-Stokes equations as described in Ref. 8; details of the current application are provided in Ref. 9. The initial grid was developed during the Pegasus design effort. Solutions of this grid required approximately 40 hr of computer time per case on a Cray-2 (Cray Research, Inc., Minneapolis, MN) computer. The grid for the postflight analysis was modified to concentrate on data in the fillet region. During the postflight analysis the surface temperatures were set to values estimated from the foil thermocouple sensors.

In a similar CFD effort, Ref. 10, the PARC code was applied to the Pegasus configuration by researchers at the University of California at Los Angeles. This code was applied at selected conditions from flights 1 and 2. A different grid system was used, although it was

tailored again to emphasize the fillet region. Solutions required approximately 50 hr of computer time per case on an IBM-9000™ (IBM Corp., Armonk, NY) computer. Details of this effort can be found in Ref. 11.

The computational solutions provided data at all locations in the flow field, and the PLOT3D interactive graphics program, Ref. 12, was used to interpret the results. Convective surface heating rates were determined from the CFD solutions using the temperature gradient between the surface and the first grid point away from the surface. The wing leading edge relative heating rates shown in this report are the temperature gradient multiplied by a constant. The relative heating rates on the fillet sidewall were divided by the value obtained at a location on the lower, forward corner of the fillet. This allows direct correlation of the data with the flight-measured relative heating rates.

RESULTS AND DISCUSSION

Vehicle Forces and Moments

The measured lift, drag, and pitching moment coefficients are shown in Fig. 6 along with the corresponding values derived from the preflight database. The overall agreement between flight and prediction is good. The incremental differences for both flights are shown to be consistent in Fig. 7.

At the lower Mach numbers, lift is lower than predicted and drag is higher than predicted. The largest discrepancies occur at the higher angles of attack at transonic speeds, where the error in lift is about 10 percent of the total. The corresponding error in drag is about 20 percent of the total. These conditions are only encountered for a few seconds and, therefore, have minimal impact on the payload performance of the Pegasus system as a whole. At higher speeds, the lift biases (flight minus predicted) are slightly positive on flight 2 and nonexistent on flight 1. The drag biases are slightly positive at all speeds.

The pitching moment flight data indicate more nose-down moment than the prediction. The errors vary during the most dynamic portions of the flight (Mach less than 2.5), which may indicate the limits of this quasi-steady analysis. At higher speeds the error is a constant level of about 0.035 which corresponds to a center of pressure bias of about 0.4 times the fuselage diameter. In turn, this corresponds to an elevator trim error of about 3°, which is within acceptable margins.

Local Aerodynamics

An example of two temperature measurements at varying depths in the wing leading edge is shown in Fig. 8. The lag between the two curves indicates the effect of the TPS in delaying the transfer of heat to the primary structure. The TPS on the wing leading edge, wing surfaces, and fillet was designed through coupled boundary layer and thermostructural analysis methods. Although the flight data indicate that the layer of ablative material was completely removed by aerothermal heating in some regions of the wing, the temperature of the primary structure was kept within its design limit of 170 °F (77 °C) until the final seconds of flight (at which point aerodynamic loads were minimal).

The relative heating rates on the leading edge at Mach 4 derived from such data are shown in Fig. 9, along with results from the F3D analysis, Ref. 9. The flight data analysis indicates that significant ablation has not begun at this flight condition. The scatter in the measured data is expected to be the result of the sensor installation. As previously discussed, the sensors were inserted during the application of thin layers of spray-on ablative, and precise control of sensor depth was not possible. The overall trend of the data indicates higher heating rates near the wing tip which would be expected because of the nature of the curved bow shock. The F3D computational solution indicates the same relative variation in heating rates, even though the modeling of the leading edge itself was very sparse.

In comparison with the wing and leading edge regions, the fillet flow field under the wing is very complex. The flow along the flat sidewall of the fillet is intersected by a shock wave generated by the wing leading edge. In addition, the flow is conditioned by the three-dimensional geometry of the circular cylinder and the transition into the flat sidewall of the fillet. The relative significance of these effects varies with the angle of attack, Mach number, and Reynolds number range encountered throughout the Pegasus flight trajectories.

During the preflight design effort, CFD methods were used to check for potential flow separation problems in this region and to provide pressure distributions for follow-on boundary-layer and TPS design methods. Flight data were used to assess other details of the CFD analysis in this region which will be discussed next.

Although the computational solutions provided data at all points on the surface and in the flow field, the flight data are available at only discrete locations. On the

other hand, the CFD data were only available at discrete times in the trajectory, whereas the flight testing provided a continuous time history of data. The combination of the two sets of data was very useful in interpreting the actual characteristics of the flow.

Figure 10 shows the relative heating rate distributions at several fuselage stations for selected flight and CFD analysis conditions. All local heating rate data have been divided by the corresponding values at the reference location shown. Typical computational distributions, such as those in Fig. 10(a), consist of two vertically separated heating rate maximums (spikes) at the forward fuselage stations (FS = 288.4 and 280.6). These appear to blend together by the most aft location shown (FS = 253.1). Computed pressure coefficients in the flow field (Fig. 11) indicate that this upper heat-flux spike is associated with the wing compression region and leading edge shock. It is felt that the lower spike is associated with the turning of the flow from the cylindrical fuselage to the flat sidewall.

The flight data for the flight 1 conditions generally confirm the location and approximate magnitude of the upper heat-flux spike at the forward fuselage stations. Agreement between the flight and computational data at the aft-most station is not consistent.

Comparison of Figs. 10(a) and 10(b), at similar Mach numbers, shows that more pronounced spikes occur in the PARC solution. This difference could be related to the differences in flight condition, the codes, or the analysis grids. At Mach 5 (Figs. 10(c) and 10(d)), the two computational solutions differ more significantly. The only difference in free-stream conditions for these cases is the Reynolds number. The available flight data are not adequate to assess the relative effectiveness of the two codes.

The pressure data also indicate that a suction region exists aft of the wing shock, that is, in the corner of the fillet sidewall and wing lower surface (Fig. 11). This suction in the computational data is associated with a corner vortex and becomes stronger at lower angles of attack. Figure 12 shows the limited flight-pressure measurements, also referenced to the forward location on the fillet, along with computational results. Both data sets show lower pressures near the wing lower surface ($z = 28$), which tends to support the existence of a corner vortex. The flight measurements show greater levels of suction than the computations at Mach 5.

CONCLUDING REMARKS

Flight measurements from the Pegasus air-launched space booster were obtained and correlated with computational data. The flight instrumentation was accommodated with minimal impact to the flight operation, and the computational results were obtained from the actual preflight design effort and a limited amount of follow-on analysis. The follow-on studies were conducted with the same level of sophistication as the design effort, relying on available codes and limited computer resources.

The correlation of vehicle forces and moments from flight and prediction was acceptable. Aerodynamic performance was slightly lower than predicted, and pitching moment was more nose-down than predicted; but these errors were within the design margins of the Pegasus system. Similarly, the aerothermal characteristics on the wing and fillet were found to be within Pegasus design limits.

Additionally, the correlations provide insight into the capabilities of the computational fluid dynamics techniques for more complex applications. Relative heating rate and pressure distributions in the complex wing body interference flow region indicate that key features were identified, despite the limitations of the computational methods (no modeling of ablation, constant wall temperatures, limited computational grid size, etc). In particular, the location and approximate magnitude of the wing shock interference heating and presence of a corner vortex were consistent in both the flight and computational fluid dynamics data. The correlations are better on the forward edge of the fillet and degrade further aft, as the flow characteristics merge. The flight data were too sparse to assess the relative effectiveness of the two codes.

ACKNOWLEDGEMENT

The authors acknowledge the Defense Advanced Research Project Agency and Orbital Sciences Corp. for their support of this research.

REFERENCES

1. Marvin, Joseph G, *Accuracy Requirements and Benchmark Experiments for CFD Validation*, NASA TM-100087, May 1988.
2. Mendenhall, Michael R., Daniel J. Lesieurte, Steven C. Caruso, Marnix F.E. Dillenius, and Gary D. Kuhn, "Aerodynamic Design of PegasusTM—Concept to Flight with CFD," in *Missile Aerodynamics*, AGARD-CP-493, 1990 (also available as AIAA 91-0190).
3. Covault, Craig, "Commercial Winged Booster to Launch Satellites from B-52," *Aviation Week and Space Technology*, vol. 128, no. 23, June 6, 1988, pp. 14–16.
4. Noffz, Gregory K, Robert E. Curry, Edward A. Haering, Jr., and Paul Kolodziej, *Aerothermal Test Results from the First Flight of the Pegasus Air-Launched Space Booster*, NASA TM-4330, 1991.
5. Noffz, Gregory K. and Robert E. Curry, "Summary of Aerothermal Test Results from the First Flight of the Pegasus Air-Launched Space Booster," AIAA-91-5046, presented at the AIAA Third International Aerospace Planes Conference, Orlando, FL, Dec. 3–5, 1991.
6. Kolodziej, Paul and Gregory K. Noffz, "Aerothermal Heating Measurements on the Pegasus Air Launched Booster," 38th International Symposium, Instrumentation Society of America, Las Vegas, NV, Apr. 1992.
7. Blackwell, B.F., R.W. Douglass, H. Wolf, and Raymond F. Giffels, "A User's Manual for the Sandia One-Dimensional Direct and Inverse Thermal (SODDIT) Code," SAND85-2478, Sandia National Laboratories, Albuquerque, NM, May 1987.
8. Ying, S.X., D. Baganoff, J.L. Steger, and L.B. Schiff, "Numerical Simulation of Unsteady, Viscous, High-Angle-of-Attack Flows Using a Partially Flux-Split Algorithm," AIAA 86-2179, Aug. 1986.
9. Kuhn, Gary D., *Postflight Aerothermodynamic Analysis of Pegasus® Using Computational Fluid Dynamics Techniques*, NASA CR-186017, March 1992.
10. Cooper, G.K. and J.R. Sirbaugh, "The PARC Code: Theory and Usage," AEDC-TR-89-15, Arnold Engineering and Development Center, Arnold AFB, TN, Dec. 1989.

11. Fricker, Darren, John Mendoza, and Ivan Catton,
A Computational Fluid Dynamics Analysis of the Hypersonic Flights of the Pegasus, NASA CR-186023, 1992.

12. Walatka, Pamela, and Pieter G. Buning, *PLOT3D User's Manual*, NASA TM-101067, 1989.

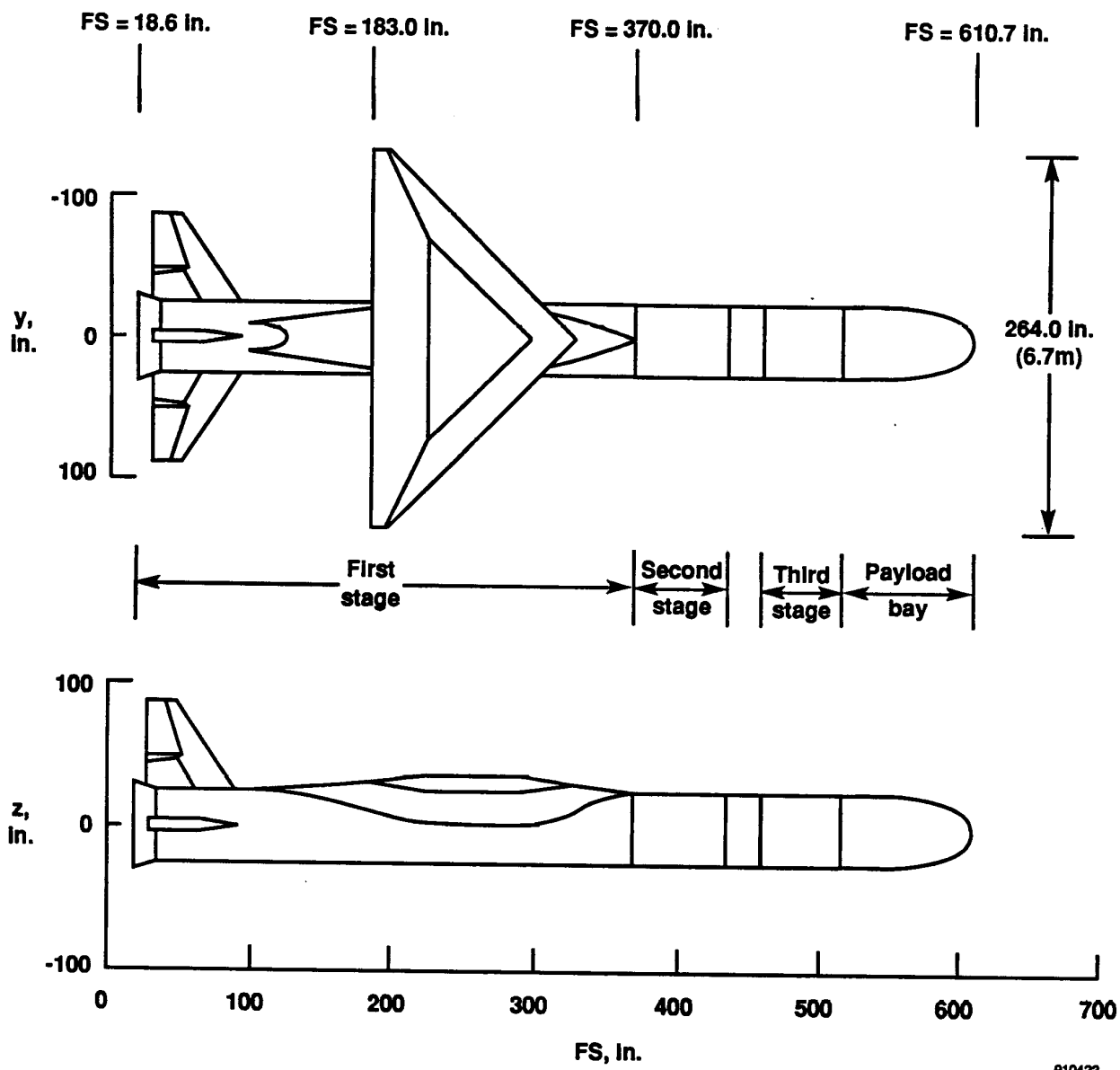
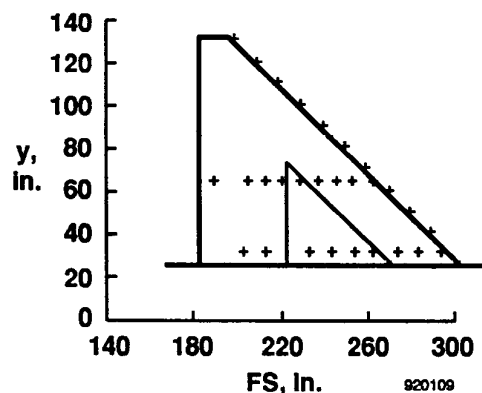
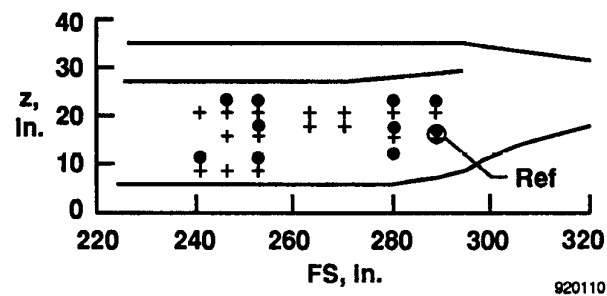


Fig. 1. Pegasus launch configuration.

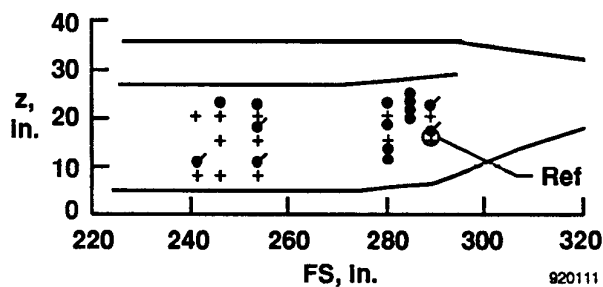


(a) Flight 1, right wing lower surface.



(b) Flight 1, right fillet sidewall.

- HRSI plug or calorimeter
- ◐ HRSI plug with pressure orifice
- + Thin foil thermocouple



(c) Flight 2, right fillet sidewall.

Fig. 2. Flight instrumentation.

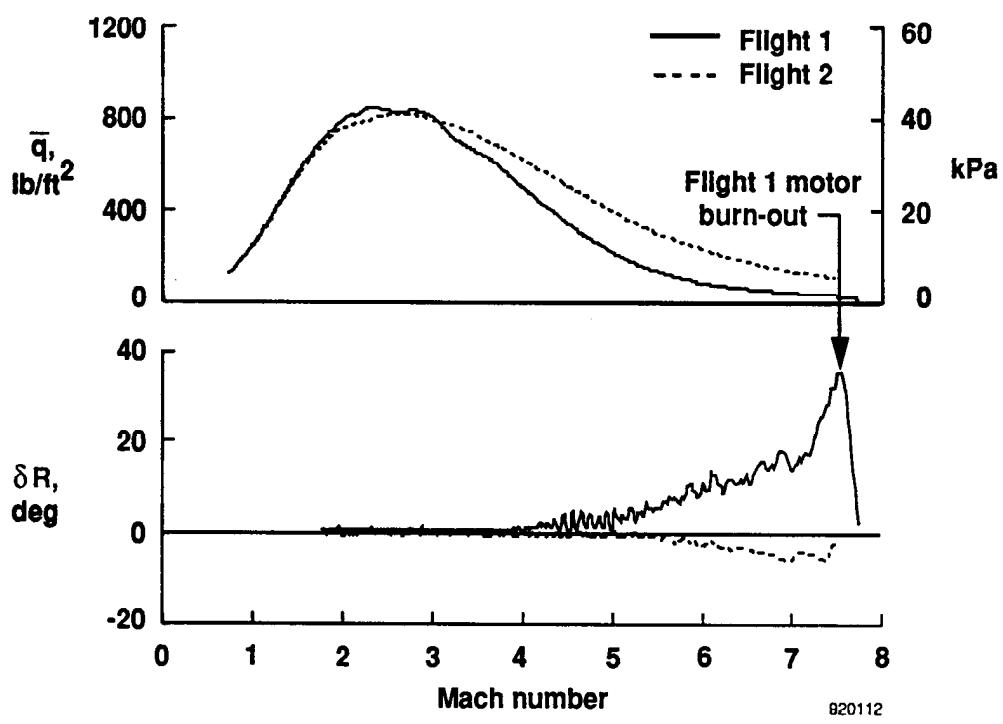


Fig. 3. Identification of thrust misalignment effects.

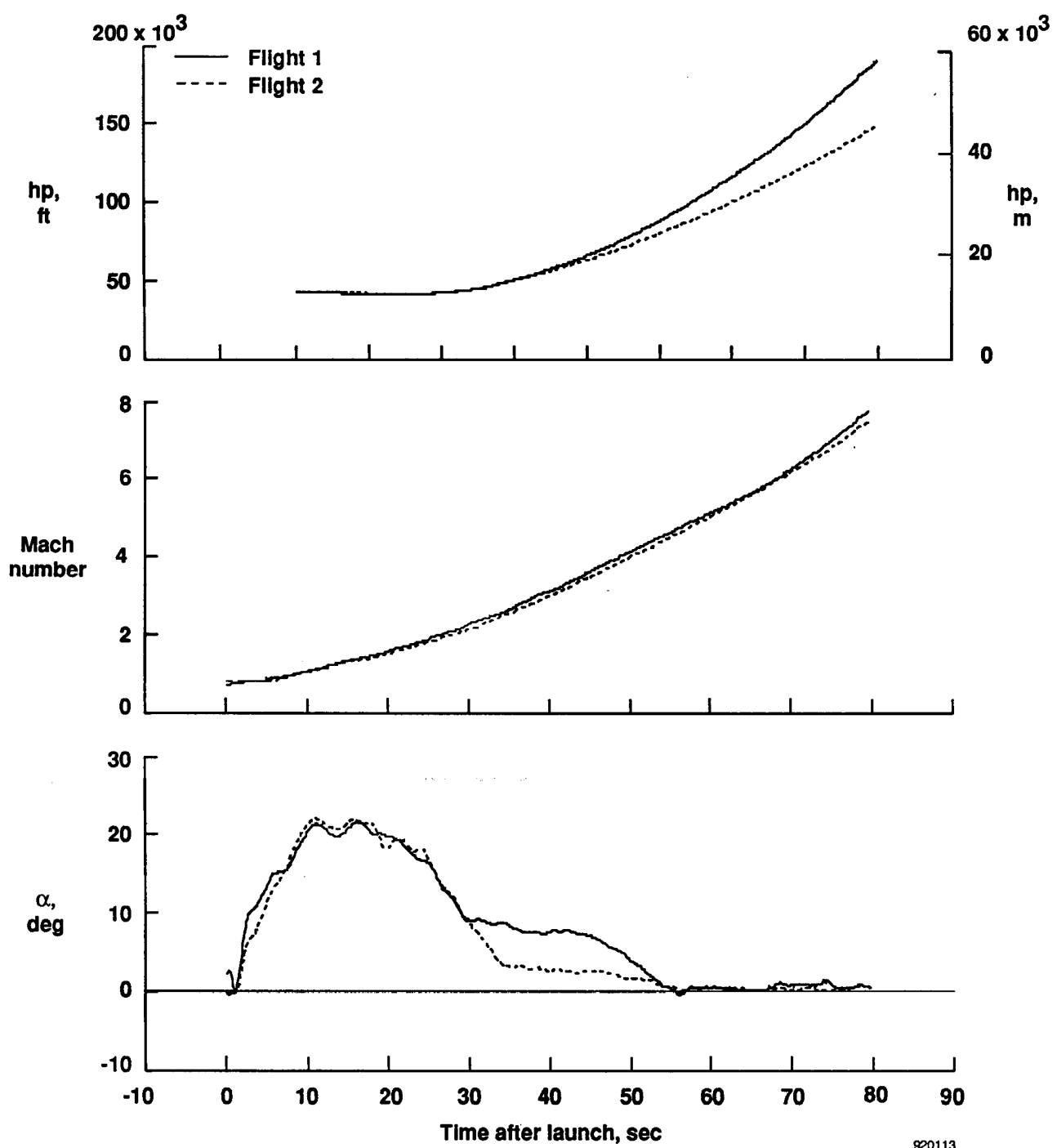


Fig. 4. Trajectory flight conditions.

920113

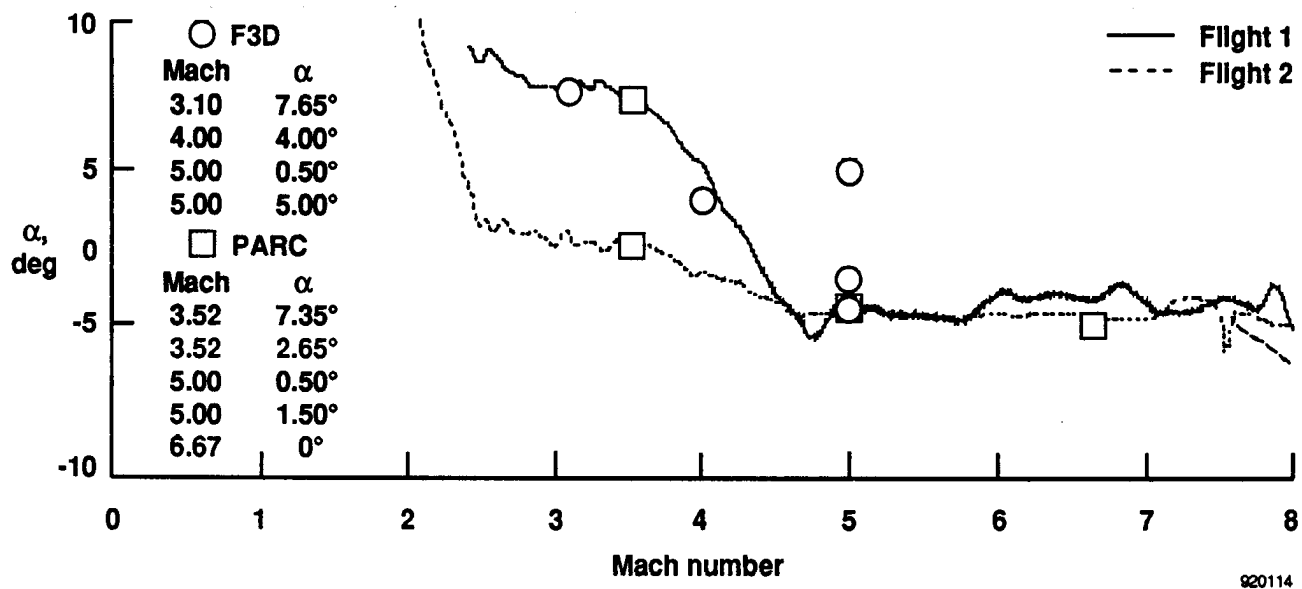
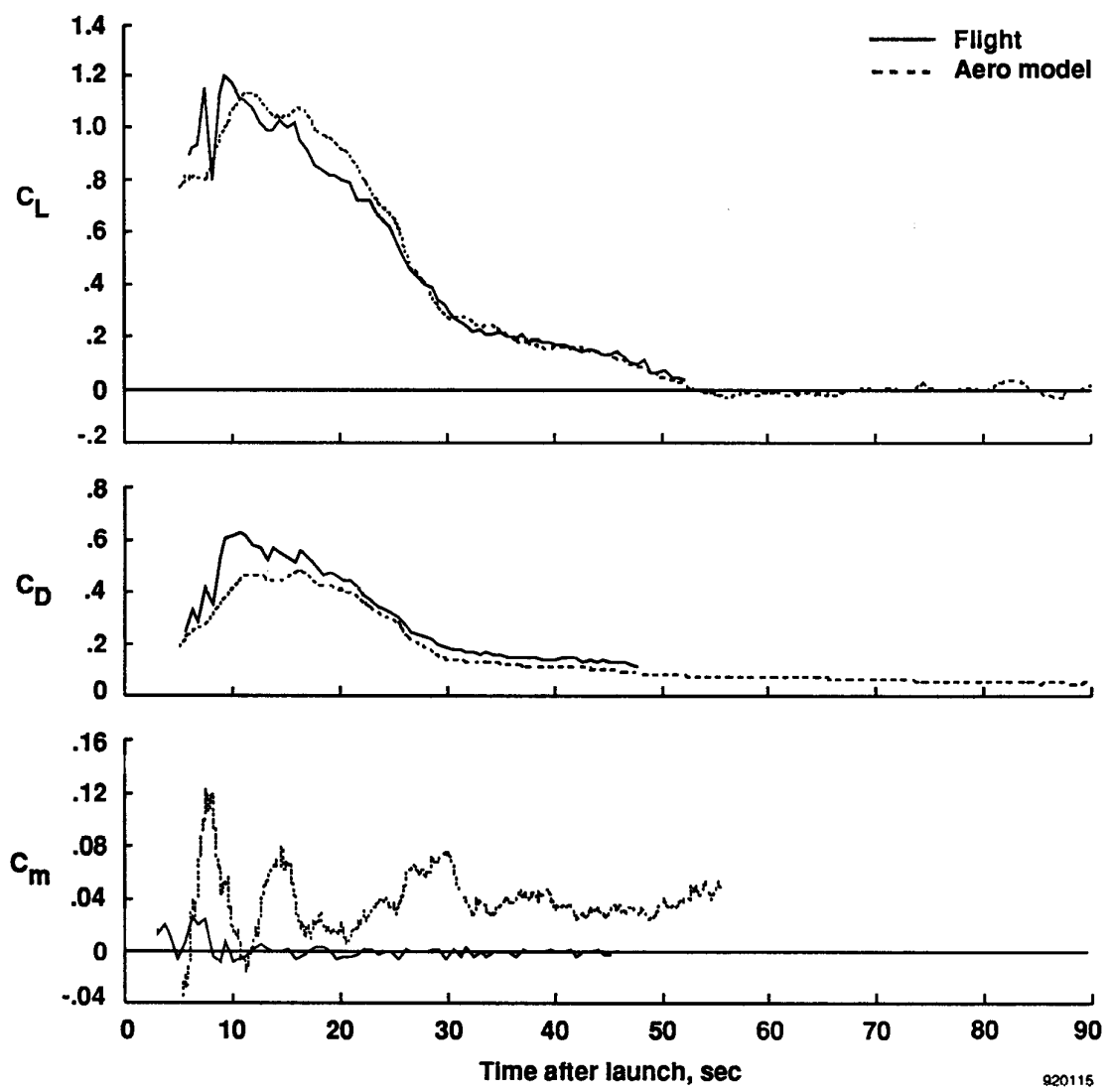
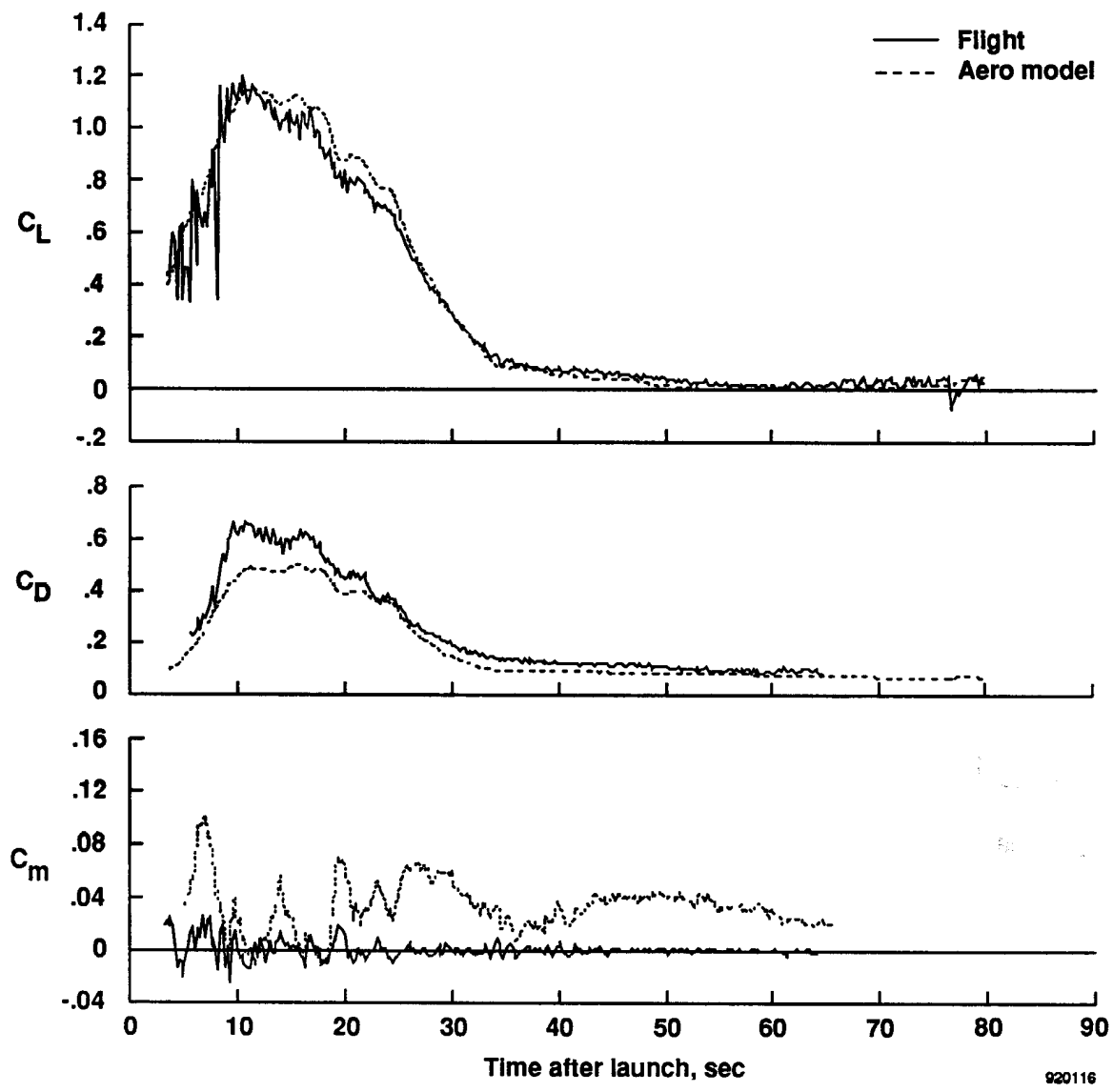


Fig. 5. High-speed computational fluid dynamics analysis flight conditions.



(a) Flight 1.

Fig. 6. Vehicle forces and moments.



(b) Flight 2.

Fig. 6. Concluded.

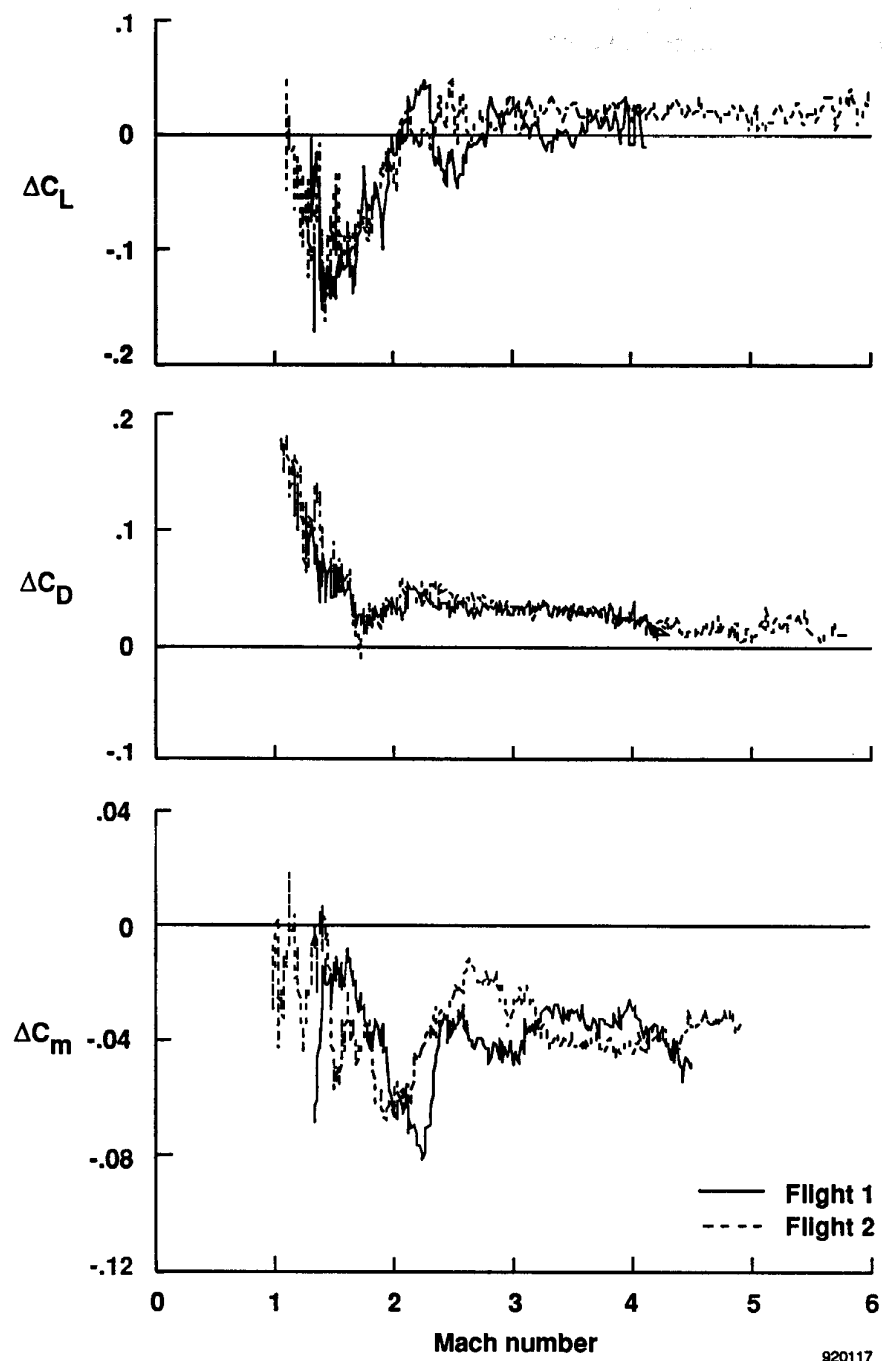


Fig. 7. Biases in vehicle aerodynamics (flight minus prediction).

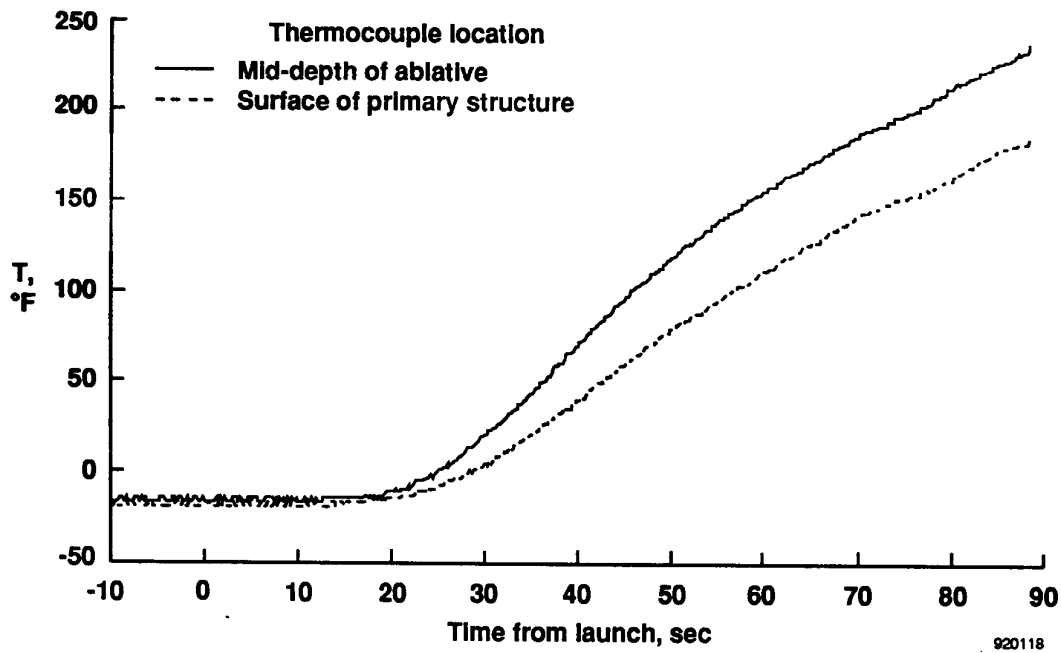


Fig. 8. Leading edge temperature time histories, $y = 65$ in.

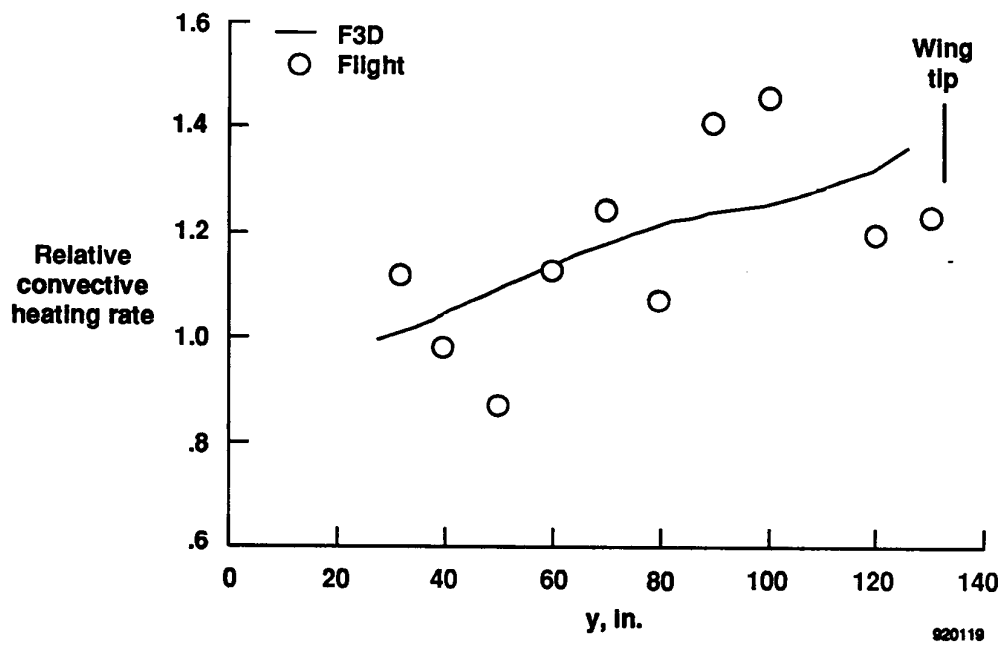
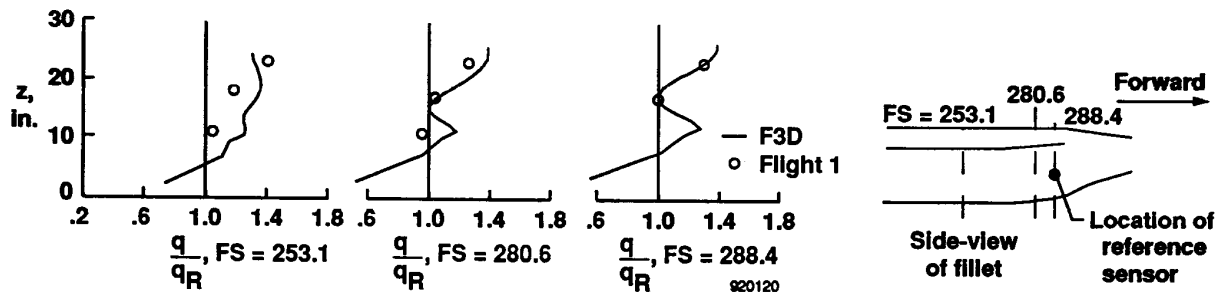
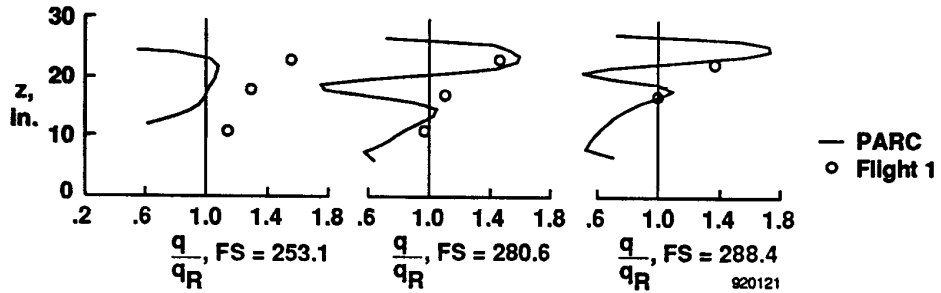


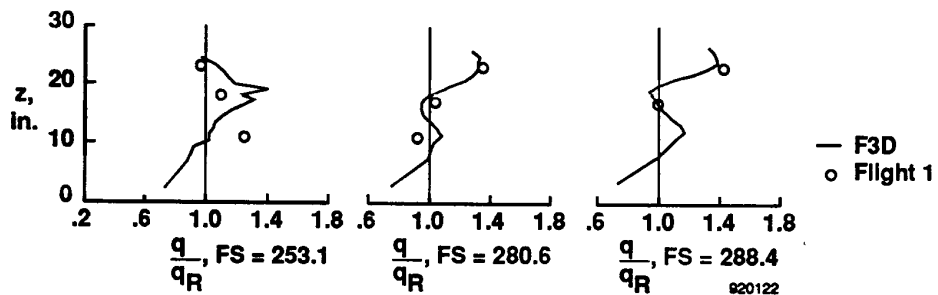
Fig. 9. Spanwise leading edge relative heating rates, Mach 4.



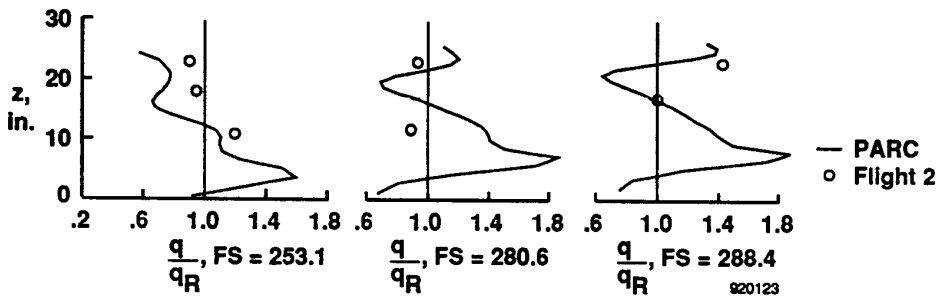
(a) $M = 3.1$, $\alpha = 7.65^\circ$, and $Re = 2.08$ million/ft (6.82 million/m).



(b) $M = 3.52$, $\alpha = 7.35^\circ$, and $Re = 1.56$ million/ft (5.12 million/m).



(c) $M = 5$, $\alpha = 0.5^\circ$, and $Re = 0.215$ million/ft (0.705 million/m).



(d) $M = 5$, $\alpha = 0.5^\circ$, and $Re = 0.404$ million/ft (1.32 million/m).

Fig. 10. Relative heating rates on the fillet sidewall.

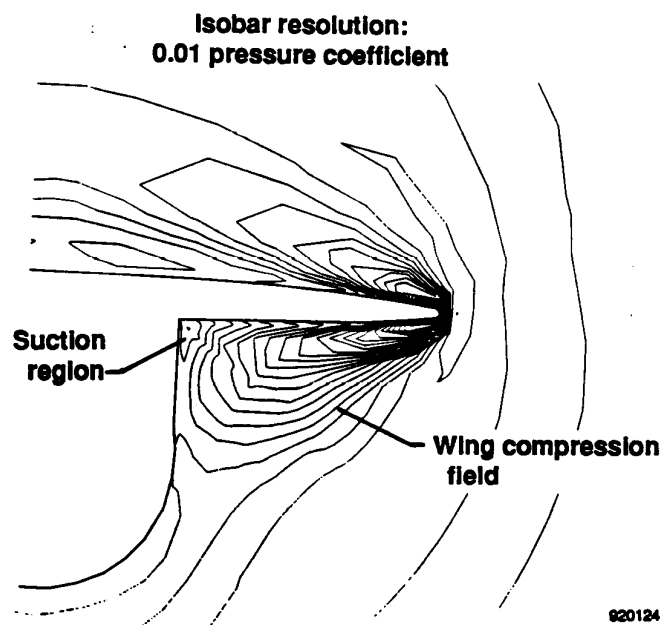


Fig. 11. Off-surface pressure field, $M = 4$, $\alpha = 4^\circ$, and $Re = 0.171$ million/ft (0.561 million/m), F3D computations, FS = 253.1 in.

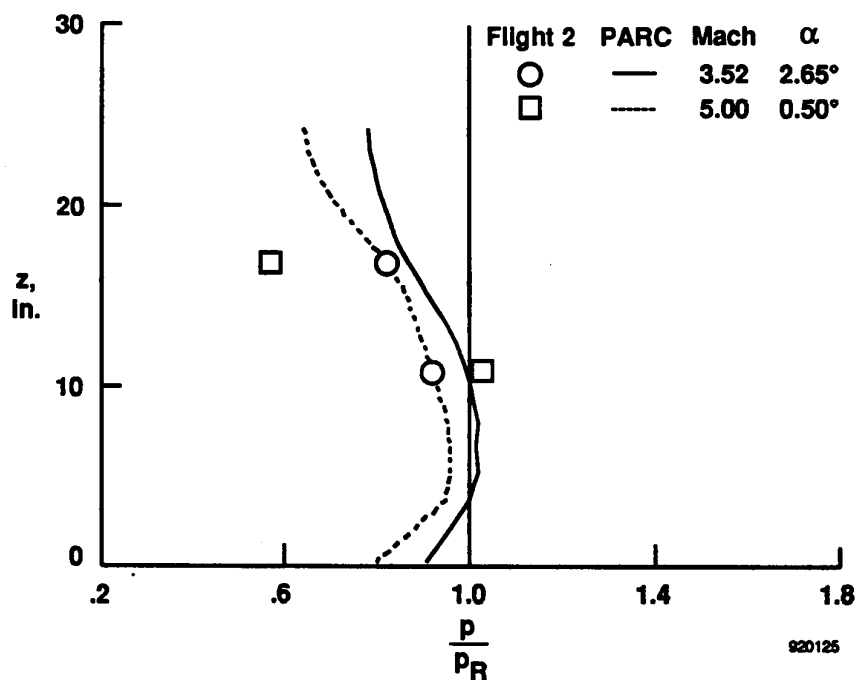


Fig. 12. Correlation of flight and computational pressure data, FS = 253.1 in.

REPORT DOCUMENTATION PAGE			Form Approved OMB No. 0704-0188
<p>Public reporting burden for this collection of information is estimated to average 1 hour per response, including the time for reviewing instructions, searching existing data sources, gathering and maintaining the data needed, and completing and reviewing the collection of information. Send comments regarding this burden estimate or any other aspect of this collection of information, including suggestions for reducing this burden, to Washington Headquarters Services, Directorate for Information Operations and Reports, 1215 Jefferson Davis Highway, Suite 1204, Arlington, VA 22202-4302, and to the Office of Management and Budget, Paperwork Reduction Project (0704-0188), Washington, DC 20503.</p>			
1. AGENCY USE ONLY (Leave blank)	2. REPORT DATE	3. REPORT TYPE AND DATES COVERED	
	April 1992	Technical Memorandum	
4. TITLE AND SUBTITLE		5. FUNDING NUMBERS	
In-Flight Evaluation of Aerodynamic Predictions of an Air-Launched Space Booster		WU-505-02-40	
6. AUTHOR(S) Robert E. Curry (Dryden Flight Research Facility, Edwards, CA), Michael R. Mendenhall (Nielsen Engineering & Research, Inc., Mountain View, CA), and Bryan Moulton (PRC Inc., Edwards, CA)			
7. PERFORMING ORGANIZATION NAME(S) AND ADDRESS(ES) NASA Dryden Flight Research Facility P.O. Box 273 Edwards, CA 93523-0273		8. PERFORMING ORGANIZATION REPORT NUMBER H-1803	
9. SPONSORING/MONITORING AGENCY NAME(S) AND ADDRESS(ES) National Aeronautics and Space Administration Washington, DC 20546-0001		10. SPONSORING/MONITORING AGENCY REPORT NUMBER NASA TM-104246	
11. SUPPLEMENTARY NOTES Prepared for the AGARD Symposium on Theoretical and Experimental Methods in Hypersonic Flows, May 4-7, 1992, Torino, Italy.			
12a. DISTRIBUTION/AVAILABILITY STATEMENT Unclassified — Unlimited Subject Category 02		12b. DISTRIBUTION CODE	
13. ABSTRACT (Maximum 200 words) Several analytical aerodynamic design tools that were applied to the Pegasus® air-launched space booster were evaluated using flight measurements. The study was limited to existing codes and was conducted with limited computational resources. The flight instrumentation was constrained to have minimal impact on the primary Pegasus missions. Where appropriate, the flight measurements were compared with computational data. Aerodynamic performance and trim data from the first two flights were correlated with predictions. Local measurements in the wing and wing-body interference region were correlated with analytical data. This complex flow region includes the effect of aerothermal heating magnification caused by the presence of a corner vortex and interaction of the wing leading edge shock and fuselage boundary layer. The operation of the first two missions indicates that the aerodynamic design approach for Pegasus was adequate, and data show that acceptable margins were available. Additionally, the correlations provide insight into the capabilities of these analytical tools for more complex vehicles in which design margins may be more stringent.			
14. SUBJECT TERMS Aerothermodynamics; Air-launched space booster; Computational fluid dynamics; Hypersonics; Wing-body aerodynamics			15. NUMBER OF PAGES 21
			16. PRICE CODE A03
17. SECURITY CLASSIFICATION OF REPORT Unclassified	18. SECURITY CLASSIFICATION OF THIS PAGE Unclassified	19. SECURITY CLASSIFICATION OF ABSTRACT Unclassified	20. LIMITATION OF ABSTRACT Unlimited